Biomaterials Science

ROYAL SOCIETY OF CHEMISTRY

REVIEW

View Article Online
View Journal | View Issue

Cite this: *Biomater. Sci.*, 2023, **11**, 7034

Mechanism and application of 3D-printed degradable bioceramic scaffolds for bone repair

Hui Lin,[a,b] Liyun Zhang,[a,b] Qiyue Zhang,[a,b] Qiang Wang,[a,b] Xue Wang*[a] and Guangqi Yan *[a]

Received 21st July 2023,
Accepted 13th September 2023

DOI: 10.1039/d3bm01214j

rsc.li/biomaterials-science

Bioceramics have attracted considerable attention in the field of bone repair because of their excellent osteogenic properties, degradability, and biocompatibility. To resolve issues regarding limited formability, recent studies have introduced 3D printing technology for the fabrication of bioceramic bone repair scaffolds. Nevertheless, the mechanisms by which bioceramics promote bone repair and clinical applications of 3D-printed bioceramic scaffolds remain elusive. This review provides an account of the fabrication methods of 3D-printed degradable bioceramic scaffolds. In addition, the types and characteristics of degradable bioceramics used in clinical and preclinical applications are summarized. We have also highlighted the osteogenic molecular mechanisms in biomaterials with the aim of providing a basis and support for future research on the clinical applications of degradable bioceramic scaffolds. Finally, new developments and potential applications of 3D-printed degradable bioceramic scaffolds are discussed with reference to experimental and theoretical studies.

1 Introduction

Bone tissues exhibit a certain degree of self-healing. For a critical bone defect with an extent of less than 2.5 cm,[1] the differentiation of bone progenitor cells into osteoblasts can result in complete bone regeneration.[2] However, extreme clinical circumstances, including high-energy injury, degenerative disease, or removal of bone tumors, can change the bone healing capacity, resulting in severe dimensional defects and bone regeneration failure.[3] Various bone repair materials have been developed to meet the growing demand for the treatment of critically sized bone defects.

Although autografts are considered the gold standard for bone grafts, they have several limitations, including donor site morbidity and limited availability.[4,5] Allografts provide a different treatment option for critically sized bone defects, but their applications are restricted owing to significant drawbacks, such as immune response complications, risk of infection, and ethical constraints.[5–7] Hence, successful scaffold designs that mimic the structure and composition of natural bone tissue are needed as alternatives to autografts for successful clinical bone repair applications. In recent years, metals, polymers, and bioceramics have been used in preclinical practice. Metals such as titanium exhibit excellent corrosion resistance and mechanical properties. However, titanium also has relatively low osteoinductivity, and an excessive difference in the elastic moduli of bone tissue and titanium exists, which leads to a stress-shielding effect around surgical sites.[8] Polymers have superior biocompatibility and biodegradability; however, their clinical applications are limited by poor osseointegration and uncontrollable degradation.[9]

Currently, bioceramics are widely applied in the field of bone repair as tissue engineering scaffolds due to their excellent biocompatibility, osteoconductive properties, and similarity to natural bone.[10,11] These materials usually bind to soft and hard tissues by forming bone-like apatite on their surfaces; therefore, they are considered bioactive.[12–15] However, biomaterials have poor mechanical properties compared to natural bone, which limits their use in filling bone defects in non-load-bearing areas, such as oral and maxillofacial areas. Furthermore, because bone defects have a variety of shapes and sizes, customizing existing biomaterials to satisfy the surgical requirements for certain bone defects is difficult.[4,16,17]

Specific structural features, such as pore size and geometry, can be controlled to a certain extent using conventional scaffold fabrication techniques; however, these features are still difficult to adapt to individualized wounds and precise scaffold structures.[18,19] In recent years, 3D-printing technology, as a pioneering manufacturing method, has been intensely studied to address these structural challenges, providing an innovative method to create porous scaffolds with improved bioactive characteristics for bone regeneration.[8–10,20,21] The preparation of bioceramic nanoparticles, their blending with

[a]*School and Hospital of Stomatology, China Medical University, Shenyang, China. E-mail: yanguangqi_1982@163.com*
[b]*Liaoning Provincial Key Laboratory of Oral Diseases, China Medical University, Shenyang, China*

other materials, or using 3D-printed customized structures allows for faster degradation of hard-to-degrade bioceramic materials such as hydroxyapatite (HA),[22,23] while degradable bioceramic materials such as tricalcium phosphate (TCP) achieve better mechanical properties and a more controlled degradation rate.[16,24] Degradable 3D-printed bioceramic scaffolds allow for the microscale structural design of customized scaffolds; when the bioceramic material degrades, a composition similar to that of bone tissue promotes bone regeneration and provides space for the growth of new bone. However, the inherently high brittleness and lack of mechanical properties of bioceramics, as well as the further weakening of the mechanical properties of the scaffold during degradation, make them unsuitable for application in bone defects in load-bearing areas[4,20] (Table 1).

During the past five years, significant advances have been made in the preclinical studies of biodegradable bioceramics for bone repair and their clinical applications. Although the clinical application of bioceramics in load-bearing bones is currently infeasible, researchers have found that the mechanical properties of existing biodegradable bioceramics are suitable for application in oral and maxillofacial bones.[61] Newly developed 3D-printing strategies and new degradable bioceramics have been used in preclinical trials for bone repair and clinical trials for bone defects, demonstrating that 3D-printed degradable bioceramics have excellent performance as substrate grafts and will have a positive impact on future treatment strategies for bone repair (Fig. 1).

The aim of this review was to summarize the 3D-printed biodegradable bioceramic scaffolds for bone repair, with a focus on the osteogenic molecular mechanisms of the scaffolds and clinical applications in the treatment of bone defects. This review also briefly discusses the existing limitations of 3D printing technology and bioceramic materials as well as the potential future development of degradable bioceramic scaffolds.

2 3D-printing techniques for bioceramic scaffolds

2.1 Stereolithography (SLA) and digital light processing (DLP)

Manufacturing methods based on light irradiation through a vat containing photocurable and bioceramic materials, resulting in plasticity by the photopolymerization of scaffolds

Table 1 Comparison of techniques for fabricating bio-ceramic bone repair scaffolds

Name	Materials	Advantages	Disadvantages	Ref.
Solvent casting and salt leaching	BG nHA TCP	Porous 3D structure Able to control pore size and porosity	Interconnected-pore structure May lead to solvent residues Irregular shaped pores	19 and 25–27
Direct Foaming	BG HA	Interconnected porosity Easy production Low cost	Irregular internal structure Fast pyrolysis	18 and 28
Freeze-drying	CS HA TCP	Preservation of the original physico-chemical and biological properties	Difficult to control porosity Long processing time	29–32
SLA/DLP	HA/PTMC PDLLA/HA TCP CS BG	High accuracy Fine internal structure achieved Increased cell survivability achieved Material saving	The viscosity of paste can influence the scaffold's reliability A long production time	33–40
SLS	nHA PCL/HA CS TCP	Controllable mechanical properties No post-processing required	High processing temperature Lower resolution	41–43
FDM	PLA/nHA PCL/HA β-TCP/HA PCL/TCP PCL/BG BG CS MgP/$SrHPO_4$	Low cost Easy to operate Controllable pore size and geometry	Limited shape and precision Bioactive factor degradation and warping of the scaffold	44–52
Inkjet printing technology	HA BG BG/HA	Low cost Material saving High resolution Fast printing speed	Risk of nozzle clogging Limited choice of materials	53–60

HA: hydroxyapatite; n-HA: nanosized hydroxyapatite; BG: bioactive glass; TCP: tricalcium phosphate; MgP: magnesium phosphate; CS: calcium silicate; PTMC: poly (trimethylene carbonate); PDLLA: poly (D, L-lactic acid); PCL: poly(epsilon-caprolactone); PLA: polylactide; SLA: stereolithography; DLP: digital light processing; SLS: selective laser sintering; FDM: fused deposition modelling.

Fig. 1 Benefits and applicable 3D printing technologies for 3D-printed degradable bio-ceramic scaffolds in bone repair.

directly on the platform, are currently popular for manufacturing bone repair scaffolds. This strategy has translated into two technologies: SLA and DLP.[33,62]

SLA is currently one of the most widely used 3D-printed technologies.[8] SLA uses a highly viscous paste as the foundation material and then employs an ultraviolet beam to selectively cure the photosensitive paste. Meanwhile, DLP features a light source that illuminates each layer simultaneously, rather than using point-by-point exposure as in SLA.[33,40] The raw materials for SLA and DLP printing scaffolds include resins (composed of monomers, photoinitiators) and additive materials.[63] The curing of scaffolds is mainly dependent on the polymerisation reaction of the resin and is not significantly affected by the addition of inorganic substances. Therefore, a broad range of bioceramics, including HA, TCP, calcium silicate (CS), and bioactive glass (BG), is available for SLA and DLP.

The main printing parameters affecting the quality of SLA printed scaffolds are curing depth (CD) and post-cure processing. CD directly affects the efficacy of photocrosslinking within and between the printed scaffold layers. It is widely agreed that CD should reach an appropriate depth. A shallow CD can lead to defects in the scaffold, and unreacted resin may pose a higher risk of cytotoxicity.[64] However, a high CD can also lead to over-curing and poor resolution of scaffold.[65] Light intensity (LI) and irradiation time (IT) are essential factors in CD.[36] The scaffolds need to be post-cured after printing to enhance the mechanical properties of the printed scaffolds, and there is a significant positive correlation between the mechanical properties and the curing time.[66] In addition, resin viscosity is also closely related to the mechanical properties and printing accuracy of light-cured scaffolds.[67] In order to ensure the precision of scaffolds in 3D printing, the viscosity of the resin needs to be reduced.[64] Research demonstrates that the resin viscosity for DLP printing should be less than 10 Pa s to prevent structure breakage[68] Adding ceramic components increases the viscosity of the resin and interfere with the light-curing process of the resin, leading to scaffold manufacturing defects.[69] Therefore, incorporating bioceramic particles places high demands on the design of SLA or DLP printed bioceramic scaffolds (Table 2).

SLA and DLP can achieve an accuracy of 50 μm.[37] The excellent accuracy allows scaffolds made using these processes contain complex internal structures and possess exceptionally high geometric resolution. β-TCP scaffolds with hollow tube structures prepared with DLP significantly promoted angiogenesis and osteogenesis.[70] In addition, customized HA composite scaffolds prepared by SLA exhibited acceptable compressive and yield strengths under both walking and running conditions and could meet loading requirements.[79] SLA and DLP

Table 2 Comparison of techniques for fabricating bio-ceramic bone repair scaffolds

Name	Material	Printing parameters	Physico-chemical characteristics	Ref.
SLA/DLP	β-TCP	IT: 6 seconds per layer Post-cure processing: dried overnight and sintered at 1150 °C for 3 h	Significantly promotes angiogenesis and osteogenic activity.	70
	HA/poly (trimethylene carbonate)	LI: 180 mW dm^{-2} IT: 9 seconds per layer Post-cure processing: The propylene carbonate diluent was removed using a gradual extraction process with propylene carbonate and ethanol mixture (1 : 1) and then replaced with 100% ethanol.	Promotes cell adhesion, proliferation and differentiation. Significantly promotes new bone formation.	36
SLS	n-HA	*d*: 1.0 mm LT: 0.2 mm ED: 2.0–5.0 J mm^{-2}	Scaffold created at 4 J mm^{-2} exhibit the highest Vickers hardness of 4 GPa and fracture toughness of 1.28 MPa.	71
	HA/PA12	*d*: 0.25 mm LP: 8W LS: 380–900 mm s^{-1} LT: 0.1 mm ED: 11.26–2.1 J mm^{-2}	Under the post-treatment at 1400 °C, the PA component disappeared from the samples and the size of the HA microcrystals was reduced to a minimum.	72
	CS	*d*: 0.8 mm LP: 5.5 W LS: 2 mm s^{-1} LT: 0.1 mm	The hydrothermally treated CS scaffolds have a nanostructured surface that provides a suitable microenvironment for cell adhesion, spreading, proliferation and differentiation.	73
FDM	PLA/n-HA	Print *T*emperatures:165 °C LT: 0.2 mm Printing speed: 60 mm s^{-1} Diameter of filament: 1.75 ± 0.05 mm	The scaffold is biocompatible and osteoinductive and can induce new bone growth *in vivo*.	74
	PDLGA/BG	Print temperatures:165 °C Diameter of filament: 1.75 mm LT: 0.25 mm Printing speed:22 mm s	Printed scaffolds containing BG have the fastest degradation rate and mechanical properties compatible with cancellous bone	75
Inkjet printing technology	BG	Viscosity of ink: 5.5–10 Pa s Nozzle diameter: 100 and 250 μm	The ink retains the 3D structure of the printed filaments. The compressive strength of the BG scaffold is comparable to that of human cortical bone.	76
	n-HA	Nozzle diameter: 210–840 μm	The reduction of the nozzle diameter reduces the number of defects in the material and improves the mechanical properties of the support.	77
	β-TCP	Viscosity of ink: 0.45 Pa s Nozzle diameter: 210, 250 and 400 μm	β-TCP slurries extruded with a nozzle diameter of 210 μm show excellent viscoelastic behavior.	78

bioceramic scaffolds offer unprecedented opportunities to design and fabricate high-precision internally structured bone repair scaffolds (Fig. 2).

2.2 Selective laser sintering (SLS)

SLS is a 3D-printing technique in which a computer-assisted CO_2 laser beam is used to selectively sinter thin layers of powder that are diffused from a powder container to the sintering platform *via* a roll, binding the materials together to form a solid structure.[42,43] The formation of an object is enabled by layer-by-layer printing of the powder material and laser irradiation, which provides great flexibility in part design and manufacturing.[12,43] However, the mechanical properties and structure of SLS-produced parts are influenced to some extent by the processing strategies and material properties.[79] HA, BG and CS are currently popular bioceramics for SLS,[73,80,81] but their printing is challenging. Research suggests that too high energy density of SLS may lead to additional phase formation or even decomposition of HA powder.[71,82] Furthermore, the high processing temperature of SLS limits the incorporation of biomaterials into the scaffolds to fabricate bioceramic scaffolds that exhibit microstructural inhomogeneity.[83] Therefore, the SLS printing parameters need to be improved to obtain bioceramic scaffolds with optimal sintering results. Laser scanning speed (LS) and laser power (LP) are critical printing parameters for SLS. The energy density (ED) of the material is directly affected by them, which in turn impacts its physico-chemical performance.[84]

Previous studies have shown that the average grain size of pure granular n-HA powders sintered at a spot diameter (d) of 1 mm and a powder layer thickness (LT) of 0.2 mm increased when the ED of SLS was increased from 2.0 J mm^{-2} to 5.0 J mm^{-2}. It is noteworthy that the sintered HA slightly decomposes and undergoes a phase transition at an energy density of 5.0 J mm^{-2}, while the nano-HA powders sintered at 4.0 J mm^{-2} exhibit the best the mechanical properties that meet the requirements of cancellous bone.[71] Recent studies have shown similar results in the fabrication of porous scaffolds using composites of HA and polyamide 12 (PA12) by SLS, where post-sintering treatments eliminated PA12 polymer from the

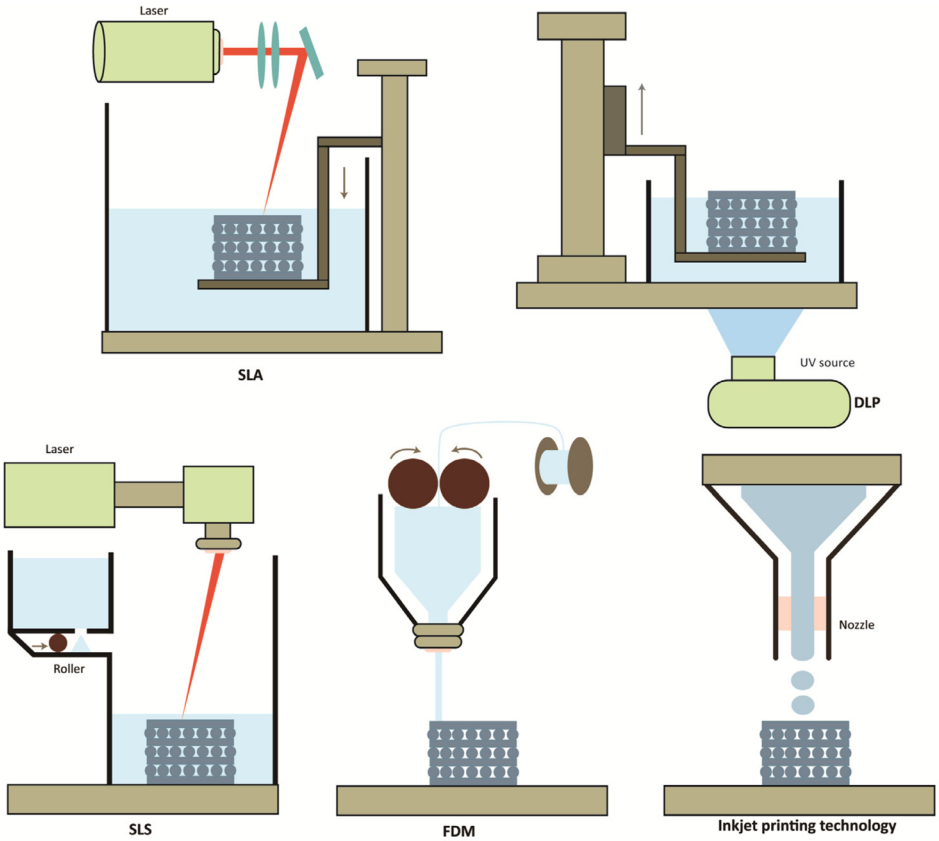

Fig. 2 Schematic diagram of the 3D process commonly used for bone engineering with bio-ceramic materials: SLA, DLP, SLS, FDM, and ink printing technology.

scaffolds and improved the relative density, crystallinity, and microcrystalline size of the parts after treatment.[72]

The high-precision nature of SLS hints at the potential of SLS for fabricating scaffolds for bone repairs. However, the current variety of printing strategies makes it more difficult to form a consensus on the ideal bone repair scaffold for bone repair. Therefore, it is necessary to develop further regarding printing parameters and material preparation.

2.3 Fused deposition modelling (FDM)

FDM is a 3D-printing technique that enables the extrusion of molten thermoplastic material in the form of continuous filaments from a small nozzle and deposition on a surface at low temperature for rapid curing at the exit.[8,52] In recent years, bio-ceramic materials such as HA, TCP, and BG have also been successfully used in FDM printing. FDM is more dependable and cost-effective when producing customized objects compared to other 3D-printing techniques and can be used to create scaffolds with controllable aperture sizes and morphologies.[51,85]

The resolution and performance of FDM-fabricated scaffolds depend on machine parameters and printing parameters.[65] Machine parameters include nozzle diameter, while printing parameters include nozzle temperature, extrusion speed and print thickness.[75,86] Researchers have explored the relationship between layer height, number of layers, raster orientation and the mechanical properties of scaffolds. The results show the highest performance when the layer height decreases due to porosity decrease and when the filaments are deposited along the longitudinal direction.[87] Moreover, the mechanical properties are lower when the number of layers increases due to increased bonding interfaces between filaments.[16,50] As for the printing temperature, setting the level too high could result in the deterioration of cells or biologically active agents and warping of the printed object as it cools.[49]

Many studies have shown that FDM-based scaffolds have excellent tunable mechanical and biochemical properties, which can be exploited for bone regeneration.[17,21,51,85] The degradable composite β-TCP scaffold formed using FDM exhibited excellent biological and mechanical properties, making it a promising candidate for bone tissue engineering.[21] However, the viscosity of the molten material and nozzle size limit the printing resolution as well as shape and precision of the objects produced by FDM compared to those produced by SLA. In the future, more studies should be conducted to evaluate the effects of many parameters on printed scaffolds' bioactivity and mechanical properties.

2.4 Inkjet printing technology

Inkjet printing is a promising method for manufacturing precision parts with customized geometries. The principle of inkjet printing is to use ceramic inks made of a mixture of non-metallic materials, dispersants, binders, and other auxiliary materials.[53] Due to the ease of making ceramic inks, bioceramic materials such as TCP and BG are widely used in inkjet printing.[76,78] Special computer-controlled nozzles eject the bioceramic ink, the individual cross-section layers are printed. These operations are then repeated in a three-dimensional manner until the required parts of all sections are bonded and stacked.[49,54]

In inkjet printing, the accuracy of the scaffold is mainly affected by the bio-ink viscosity and the nozzle diameter.[88] Studies have demonstrated that the viscosity of ink should be low enough (<10 Pa s) to form uniform droplets during the jetting process and have sufficient rheology.[89] Meanwhile, nozzle diameter has been found to affect the mechanical properties.[77] Recently, inkjet-based printing technologies have been used to prepare high-performance 3D-printed scaffolds. Combined with fast and efficient manufacturing, inkjet printing allows the production of complex-shaped ceramics with precise geometries and decreases material waste.[55,56] Studies have shown that pure BG scaffolds or BG composite scaffolds for drug loading not only lead to favorable osteogenic quality but also to a significant increase in cellular alkaline phosphatase (ALP) activity.[57] The main limitation of this printing technology is the need for excellent ceramic ink stability and the nozzles to remain unobstructed during the printing process. The ideal ink droplets must have a uniform shape and density, no droplet splash, and no "satellite droplets".[58,59] The non-metallic particles in the ceramic ink must be sufficiently small to avoid clogging of the nozzles during or after the jetting process.[54,60]

3 3D-printed degradable bioceramic scaffolds

3.1 HA scaffolds

HA, a bioceramic with an inorganic composition close to that of bone, has excellent biocompatibility and osteoconductivity; therefore, HA is frequently employed in clinical practice to repair bone defects.[85] Despite the good osteogenic properties of HA scaffolds, their main drawback is that their biodegradation is difficult, which significantly limits the formation of new bone at the scaffold implantation site.[4]

The degradation mechanisms of bioceramic scaffolds implanted in the body include solubility degradation and cell-mediated biodegradation.[90] The solubility degradation of a scaffold primarily depends on its physico-chemical properties and structural design. Cells that participate in cell-mediated biodegradation, such as macrophages and osteoclasts, play a key role in determining the fate of bioceramics, especially calcium phosphate materials, as these cells play a vital role in material resorption and osteogenesis.[12,14,91] Researchers have progressively investigated degradation strategies for HA scaffolds.

Biodegradable HA scaffolds not only produce molecules to regulate the microenvironment of bone regeneration but also allow new bone to grow inward.[10,85,92] The current prevailing modification methods for increasing the biodegradability of HA scaffolds include mixing HA scaffolds with degradable substances or utilizing nanosized hydroxyapatite (n-HA) materials to prepare implant scaffolds.[23,51,79] The combination of easily degradable materials with HA has resulted in satisfactory degradation rates.[93,94] Owing to the nanoscale particle size (≤100 nm) and extensive surface area of the n-HA material, the n-HA scaffold can lead to relatively rapid degradation and accelerated substitution of the scaffold with bone tissue.[23,95,96] In addition, n-HA is hydrophilic and promotes water penetration into the matrix, thereby accelerating scaffold degradation.[51] Polylactide (PLA)/n-HA scaffolds with a homogeneous dispersion of n-HA particles prepared by FDM were confirmed to have good biocompatibility and drug loading. Rabbit model experiments showed that this scaffold has great potential for repairing critical bone defects.[97] This result is supported by subsequent research studies, which revealed that increasing the HA content of the composite scaffold within an effective concentration range did not significantly affect the mechanical strength of the scaffold but enhanced osteogenesis *in vivo*.[51,98] Applying degradable HA in 3D printing offers improved bioactive properties and more suitable degradation rates for tissue engineering solutions, demonstrating the great potential of degradable HA in applications for bone repair. However, most current research on degradable HA scaffolds is based on preclinical studies. Further investigations and clinical testing are required for the clinical application of HA scaffolds in bone repair.

3.2 BG scaffolds

Professor Hench developed the first BG material in the early 1970s based on a SiO_2 (45%)–Na_2O(24.5%)–CaO(24.5%)–P_2O_5(6%) system.[8,99,100] BG is a promising material for clinical bone repair because of its excellent mechanical strength and biocompatibility. More importantly, the controlled degradation rate of BG also provides space and favorable factors for new bone formation[101] (Table 3).

BG does not degrade *in vivo via* the same mechanism as that of HA materials; BG degrades mainly through dissolution.

Table 3 Physical properties of biodegradable bio-ceramic materials

Material	Compressive strength (MPa)	Young's modulus (GPa)	Dissolution behavior	Ref.
HA	4–60	20–55	Very slow	91, 92 and 102
BG	70	16.0–16.4	Moderate	47 and 101
TCP	2–17.94	1.48	Moderate	102 and 103
MP	5–6	11.9–12.1	Rapid	14, 104 and 105
CS	6.08–19.44	70.7–75	Rapid	106 and 107
Cortical bone	90–230	5–23	—	92
Cancellous bone	2–45	0.1–4.5	—	92

Partial dissolution of the glass surface occurs first because of ion dissolution, which triggers the formation of a silica-rich layer; finally, an apatite layer forms.[108,109] The ions released by the dissolution of the BG surface control the phenotypic transformation of macrophages and their production of cytokines, chemokines, and growth factors, thus creating an ideal microenvironment for implant-site osteogenesis and angiogenesis.[110]

One of the major advantages of BG scaffolds is the use of hybrid scaffold materials consisting of BG and other materials. The 3D-printed composite scaffolds with different ratios (5, 10, and 20 wt%) of BG had higher hydrophilicity and compressive strength than pure poly(epsilon-caprolactone) (PCL) scaffolds, and the increased hydrophilicity of the scaffolds further enhanced cell adhesion and proliferation.[48] Designing a new BG scaffold structure for bone repair is another common method for modifying BG scaffolds. Previous studies demonstrated that altering the scaffold pore geometry and porosity can regulate cell adhesion, proliferation, and differentiation.[111] Pores with different sizes, such as macropores (>50 μm) and micropores (<10 μm), can facilitate cell migration and ion exchange between the scaffold and environment, respectively.[111,112]

Although BG materials show great promise for bone tissue regeneration, most current research on BG is based on preclinical investigations. Only a few clinical studies have reported the clinical application of BG materials, such as 45S5 BG, S53P4 BG, and borate-based BG compositions (13-93B3), in bone repair.[113–119] Further investigations are required to understand the potential of 3D-printed BG scaffolds for application in repairing bone defects. Overall, the clinical application of 3D-printed BG scaffolds for bone defects remains limited. Overall, the use of 3D-printed BG scaffolds for bone defects in clinical applications is currently limited. Further translational studies are necessary.

3.3 TCP scaffolds

TCP is a representative bioceramic material that has an inorganic composition similar to that of bone[11,120] as well as ideal structural, mechanical, biocompatibility, and osteoinductive qualities.[10,121] The TCP degradation process includes both solution degradation and cell-mediated biodegradation. Foam-like TCP scaffolds with concave pores have been found to have a faster degradation rate because more osteoclasts can be formed and collected.[122] This result agrees with the opinions of subsequent researchers.[91]

Improving 3D-printed technology and developing new composite materials for applications are central goals for promoting the bone regeneration potential of TCP scaffolds. A PCL/β-TCP cross-scale scaffold created by combining meltelectrowriting and FDM 3D-printed methods provides a stable environment for cell growth in the thick fibers as well as a connecting bridge for cell growth in the thin fibers, allowing cells to form bone in the pores of the scaffold. Furthermore, *in vitro* experiments revealed that the Ca^{2+} and PO_4^{3-} provided by β-TCP lysis in the composite significantly encouraged osteogenic differentiation of the bone marrow mesenchymal stromal cells (BMSCs) on the scaffold, significantly improving its osteogenic performance.[46]

Recently, the drug-delivery potential of CP scaffolds has attracted considerable attention. A 3D-printed novel drug-loaded porous scaffold allowed for controlled drug loading and release curves and was found to have antimicrobial and bone-regenerative properties with low cytotoxicity.[120] TCP scaffolds with dual drug delivery capabilities have also attracted attention. A release system consisting of the rapid release of one drug and sustained release of another improved *in vitro* angiogenesis and enhanced osteogenic differentiation.[123]

The biodegradable behaviour of TCP has received increasing attention. However, bone tissue engineering scaffolds built from pure TCP alone have thus far been unable to achieve the desired degradation rates and mechanical qualities necessary for bone regeneration despite their good biocompatibility and osteoconductivity.[103] Therefore, creating composite TCP scaffolds with equivalent degradation and bone formation rates as well as other additional features is needed for the regeneration of bone defects.

3.4 Magnesium phosphate (MgP) scaffold

Recently, fully bioresorbable MgP-based bioceramic materials have attracted significant interest. MgP materials are biocompatible and biodegradable, allowing bone healing while delivering magnesium ions to the bone repair microenvironment. MgP can be used as a component in composite implants for bone lifting. Histological investigations have shown that MgP/PCL scaffold are embedded and integrated into newly formed bone, demonstrating that this biphasic ceramic material can be successfully used as a graft substitute.[45]

The *in vivo* degradation of MgP materials can be broadly divided into dissolution degradation and cell-mediated degradation; however, in recent years, researchers have found the presence of osteoclasts in animal experiments, suggesting that biolysis may occupy a more critical position.[124] Overall, the degradation process and osteogenesis of MgP scaffolds *in vivo* are still poorly understood compared with those of other biodegradable bioceramic materials. Studies have shown that high concentrations of Mg ions are cytotoxic and prevent the formation of new bone.[44,124] Recent studies have shown that 3D-printed MgP scaffolds exhibit higher cell activity than TCP *in vitro* experiments, suggesting a far-reaching future for MgP scaffolds in bone repair applications.[14] However, *in vivo* degradation is a complex process that depends on various factors such as pore size, porosity and side of implantation. *In vitro* experiments can only be approximated due to the lack of cellular presence. Therefore, future *in vivo* studies are needed to confirm the experimental results further.

3.5 CS scaffold

CS materials have emerged as promising bone substitute materials. CS ceramic materials possess better mechanical properties and faster degradation rates than those of HA and

phosphate-based materials.[11,107,125] The *in vivo* degradation rate of CS materials is similar to those of the bioceramic materials mentioned above and involves both dissolution and cell-mediated degradation processes. However, some researchers have found that dissolution degradation may be more prevalent *in vivo* given that CS ceramics have better solubility than other potential scaffold materials.[126,127]

In recent years, there has been increasing research on composite scaffolds made from CS doped with other biomaterials, many of which have shown promise for bone repair, good biocompatibility, and excellent degradability.[126] Magnesium-doped CS 3D-printed scaffolds exhibited superior mechanical properties to those of pure CS scaffolds. Histological analysis of cranial bone specimens *in vivo* showed that the CS composite scaffold had a higher osteogenic capacity than the pure CS scaffold at 8 and 12 weeks.[128]

CS-based ceramics have been shown to have good osteogenic and mechanical properties, similar to those of human bone tissue. However, their faster degradation rate than the regeneration rate of bone tissue may limit their application on bone repair. The researchers prepared ZrO_2/CS composite scaffolds using the DLP technique. Their findings indicated that as the CS content increased, the aggregated CS interconnected and formed a stable support structure, increasing the composite scaffolds' compressive strength. Also, the CS spread area on the scaffold surface increased, and the degradation rate increased.[129] Hence, exploit the beneficial effects of the released calcium and silica ions, the design of calcium silicate ceramic materials with controlled degradation may be a future development direction.

4. Immune-inflammatory response to 3D-printed degradable bioceramic scaffolds

4.1 Acute inflammatory stage

In body-implant-mediated immune and osteogenic responses, macrophages have received the most attention because of their plasticity and multiple roles in the overall process.[130] During the initial stage of bioceramic scaffold placement at the site of bone trauma, a hematoma forms near the scaffold, and the interaction between blood and scaffold triggers an acute inflammation characterized by neutrophil and macrophage recruitment.[131,132] Macrophages are polarized towards the pro-inflammatory phenotype, M1 macrophages, by lipopolysaccharide and interferon-γ (IFN-γ) in the inflammatory microenvironment. Researchers generally believe that M1 macrophages regulate osteoclast activation and kill pathogens by releasing pro-inflammatory factors such as tumor necrosis factor-α (TNF-α), interleukin-1β (IL-1β), and interleukin-12 (IL-12), thus acting as anti-infective and removing excess matrix.[131,133–136] Research claimed that β-TCP can drive macrophage differentiation towards the M1 phenotype, whereas HA drives macrophages more towards the M2 phenotype. The high pro-inflammatory factors secreted by β-TCP-induced M1 macrophages may prolong inflammation and enhance the immune response. In contrast, HA may result in lower levels of inflammation compared to β-TCP, suggesting the superiority of HA in providing a local environment suitable for initiating bone formation.[137] A dose-dependent effect of BG was also observed on macrophage polarization. Low concentrations of BG promoted macrophage conversion to the M2 phenotype, whereas high concentrations of BG particles increased the number of the M1 macrophage, thereby slowing wound healing.[138] However, in recent years, it has been shown that M1 macrophages not only induce mesenchymal stem cells (MSCs) to form osteoblasts by producing oncostatin M (OSM) and cyclooxygenase-2 (COX-2) but also promote endothelial cells to upregulate genes associated with sprouting angiogenesis,[139–141] suggesting that an initial inflammatory response, predominantly by M1 macrophages, is necessary for optimal fracture healing.

4.2 Bone formation stage

The phases of bone repair are consecutive but partially overlapping.[142] Thus, before the end of the inflammatory phase, the site of degradable bioceramic scaffold placement also initiates the process of cartilage formation and replacement by bone trabeculae. Anti-inflammatory phenotype M2 macrophages are actively involved in the post-inflammatory repair phase at the site of bioceramic scaffold implantation.[143] On the one hand, M2 macrophages can secrete platelet-derived growth factor (PDGF), vascular endothelial growth factor (VEGF) and related enzymes to enhance early angiogenesis and the coupling between angiogenesis and osteogenesis.[144,145] On the other hand, M2 macrophages induce the secretion of transforming growth factor-β (TGF-β) and bone morphogenetic protein-2 (BMP-2), which in turn induces osteogenic Differentiation.[146] It has been shown that silica ions produced by CS degradation can directly induce M2 polarization.[147] Furthermore, CS ion products significantly enhance the secretion of immunosuppressive factors in hBMSCs, which are activated to stimulate M2 macrophage polarization.[148]

Notably, during the bone repair phase, it is one-sided to assume that M1 macrophages inhibit new osteogenesis while M2 macrophages promote osteogenesis. The interaction between different phenotypes of macrophages and the organism can effectively regulate the behavior of osteogenesis-associated cells, which play a crucial role in bone remodeling. Research showed that M1 macrophages can promote the proliferation and differentiation of osteoclasts through the secretion of TNF-α,[149] whereas M2 macrophages are associated with matrix mineralization of BMSCs.[150] Therefore, it is possible to achieve optical bone repair by properly regulating macrophage polarization during implanting of a bioceramic scaffold.

5 Bioceramic scaffold-induced pathway modulation for bone repair

5.1 Mitogen-activated protein kinase (MAPK) signaling pathway

MAPKs are a group of serine/threonine kinases primarily involved in cell proliferation in response to external stimuli.

Extracellular stimulation leads to the activation of a signaling cascade consisting of MAPK, MAPK kinase, and MAPK kinase kinase.[151] These three kinases are sequentially activated and regulate the downstream pathways. There are three well-studied MAPK osteogenic branching pathways, extracellular-signal-regulated kinase (ERK), c-Jun N-terminal kinase (JNK), and p38.[152] The JNK and p38 pathways have similar functions in inflammation, apoptosis, and growth, while the ERK pathway mainly regulates cell growth and differentiation.[153,154]

The role of HA in promoting osteogenic differentiation at the defect site during bone repair has been uncovered gradually.[90] n-HA was shown to accelerate the expression of osteogenic genes in osteoblast lineage cells compared with micron-sized HA.[155,156] The application of n-HA promoted osteopontin (OPN) expression and decreased ALP expression in BMSCs and MC3T3-E1 cells. The ERK signaling pathway mediated these effects by stimulating the expression of the specific signaling proteins fibroblast growth factor receptor substrate 2 (Frs2α) and ERK1/2 through the cell surface, that is, phosphate transporters and fibroblast growth factor (Fgf) receptors, and subsequently stimulated the downstream protein expression of OPN and ALP.[157]

Many studies have suggested that Mg^{2+} may be essential to promoting bone regeneration through MAPK signaling pathways, including the ERK1/2 and p38 signaling pathways.[158] Researchers found that Mg^{2+} activates the ERK/MAPK and p38/MAPK pathways, stimulating osteogenic differentiation.[159,160] Li *et al.* also showed that Mg^{2+} could upregulate Runx2 transcription in BMSCs by targeting the ERK1/2 and p38 MAPK pathways.[161] This is consistent with the findings of Lin, who found that Mg^{2+} selectively activated the ERK/MAPK pathway.[159]

Researchers have found that a critical characteristic of CS is its tendency to release ions at concentrations that promote osteoblast proliferation and differentiation.[107] Further studies found that CS can promote osteogenesis through the MAPK pathway (including the p38, ERK, and JNK subfamilies), especially encouraging the expression of Collagen I (COL-I), a2b1 sub integrin, ALP, and osteocalcin (OCN), and silicon ions increased ERK and p38 activity in a dose-dependent manner.[162–165] Interestingly, some researchers have suggested that CS does not affect JNK activity.[162] However, a subsequent study showed that CS induced a pro-inflammatory response *via* a the toll-like receptor 2 (TLR2)-mediated JNK pathway in a mouse RAW 264.7 macrophage line.[166]

5.2 Bone morphogenetic protein (BMP) signaling pathway

BMPs are members of the TGF-beta superfamily and play an important role in bone formation and stem cell differentiation.[167] Two types of BMPs exist: receptor type I (BMPR-I) and type II (BMPR-II). BMPs bind to receptors on the cell membrane and initiate signaling.[168] BMPR-II phosphorylates BMPR-I, which in turn phosphorylates the small mother against decapentaplegic (Smad) protein.[169] The Smad protein then initiates a series of phosphorylation events in the Smad complex and forms a complex with runt-related transcription factor 2 (Runx2), a key osteogenic transcription factor, controlling osteogenesis-related genes such as osterix (OSX) and OCN to direct transcriptional activity.[170,171]

Bioceramics are thought to activate the BMP signaling pathway. BMSCs cultured with HA showed significantly increased mRNA expression levels of BMP2 and BMP4. Smad1, Smad4, Smad5, and distal-free homologous frame 5 (Dlx5), macromolecules of the Smad signaling pathway downstream of BMP signaling, were also upregulated.[172] This result is consistent with that of Wang *et al.*, who found that n-HA facilitates cell adhesion and osteogenic differentiation of BMSC, which can be attributed to the activation of the BMP/Smad signaling pathway.[173] Similar osteogenic mechanisms have been identified and β-TCP has been shown to regulate BMP2 expression in macrophages. The released BMP2 binds to BMPR2, thereby activating Smad5. Activated Smad5 forms a complex with Smad4 and translocates to the nucleus. The complex then promotes the expression of Dlx5 and induces the expression of Runx2, leading to osteogenic differentiation of BMSCs.[174]

CS ceramics have been found to significantly enhance osteoblast migration and differentiation. *In vitro* and *in vivo* experiments revealed that CS bioceramics activate BMP signaling pathways and induce downstream cascades of bone morphogenetic proteins (OCN, OPN, and Runx2).[175] CS induces the accumulation of phosphorylated Smad1/5.[100] Follow-up experiments further revealed that CS mediated migration and osteoblast differentiation. Furthermore, downstream cascades of bone morphogenetic proteins are significantly downregulated by the inhibition of BMP2 activity.[176]

5.3 Wingless/integrated (Wnt)/β-catenin signaling pathway

The Wnt signaling pathway is important for osteoblast differentiation and bone development in MSCs. In the classical Wnt signaling pathway, Wnt ligands bind to the Frizzled receptor and low-density lipoprotein receptor-related protein 5 (LRP5) and low-density lipoprotein receptor-related protein 6 (LRP6), which prevent the phosphorylation and degradation of β-linked proteins and thus promote osteogenic gene expression.[100,177] Degradable bioceramics can activate the classical Wnt/β-catenin signaling pathway by releasing corresponding ions, thereby facilitating bone repair. Activation of the Wnt/β-catenin signaling pathway may occur during the degradation of bio-ceramics containing calcium, phosphate, and silicate ions, thereby regulating the expression of ALP, OPN, COL1, and OCN.[178–180]

A significant increase in cellular β-catenin-related mRNA and protein levels was observed after culturing hBMSCs with strontium-substituted BG. In contrast, samples pretreated with Wnt signaling pathway inhibitors showed complete blockage of β-catenin, dickkopf-1 (DKK1), and Wnt5a expression.[181] A more in-depth study was conducted to explore the molecular processes involved in activating the Wnt/β-catenin signaling pathway for osteogenesis using boron-containing mesoporous BG scaffolds. Researchers found that transcription factor 7-like 2, which is located downstream of the Wnt/β-catenin signaling pathway, could induce the upregulation of lipocalin-2 (LCN2)

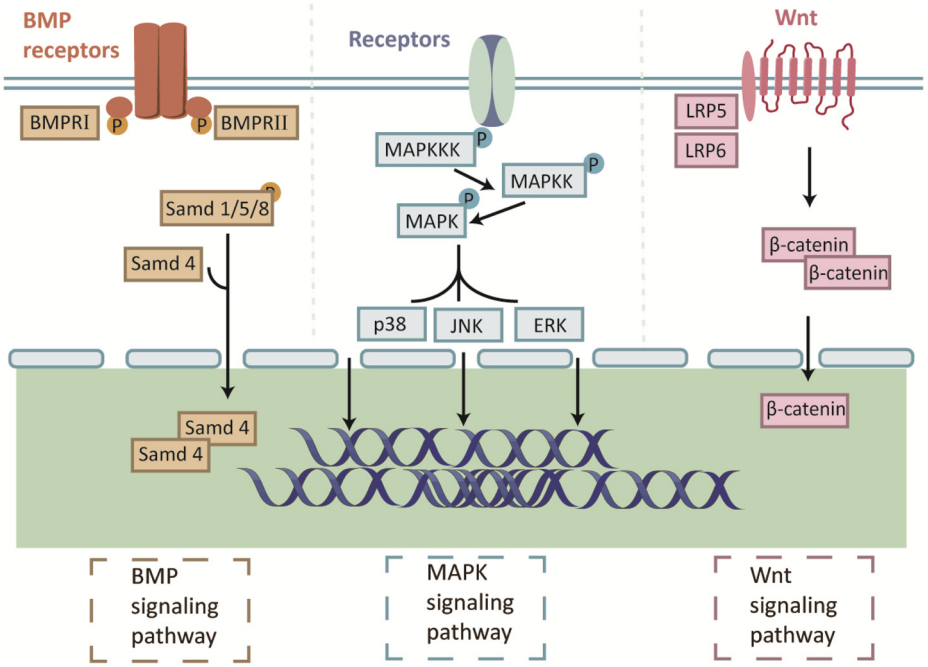

Fig. 3 Illustrations of the classic cellular pathways of bio-ceramic.

expression in osteoblasts, thereby improving osteogenic differentiation[182] (Fig. 3).

5.4 Other discovered signaling pathways

Recently, new pathways through which BG materials promote bone repair have been identified. Li-MBG reverses high glucose-induced proliferation, migration, and osteogenic differentiation of BMSCs by upregulating Integrin α3 and activating the β-catenin/transcription factor 7 (Tcf7)/cellular communication network factor 4 (Ccn4) signaling pathway.[183] Some researchers have found that BG cross-linked to hydrogels can promote osteogenesis by activating the Runx2/Bone gamma-carboxyglutamate protein (Bglap) pathway. However, the mechanism by which this material activates the Runx2 upstream signaling pathway is not clear and further research is needed.[184]

Studies have shown that dissolved calcium and phosphorus ions are non-toxic to the human body and encourage bone cell proliferation and differentiation, enabling bone defect repair.[185,186] Therefore, one possible mechanism by which TCP regulates osteogenesis is that TCP can promote osteoblast differentiation *via* the release of ionic components. Calcium ions have been proposed to activate the calmodulin and calmodulin-dependent kinase II (CaM-CaMKII) pathways, thereby promoting osteoblast differentiation.[187] ERK, JNK, p38, and cAMP response element binding Protein (CREB) are important CaMKII (δ) downstream molecules. Calcium ions activate CaMKII (δ), leading to the phosphorylation of ERK, JNK, and p38. ERK and JNK activate activator protein-1 (AP-1) through fos proto-oncogene (c-Fos) and c-Jun, respectively. AP-1 activates the nuclear factor of activated T cells c1 (NFATc1) expression, leading to osteoclast formation in many osteoblasts.[188] In addition, calcium ions can also flow into the downstream MAPK, Wnt, and BMP-2 signaling pathways, thereby promoting the expression of osteogenic differentiation-related genes.[174,189,190] This result is consistent with subsequent experiments.[179] Recently, a novel mechanism by which calcium phosphate promotes osteogenesis was proposed. Ca/P ratios in calcium phosphate can effectively promote the receptor activator of nuclear factor-kappaB ligand (RANKL)-RANK binding and trigger activated nuclear factor-kappaB (NF-κB) signaling, leading to dramatic osteoclast differentiation.[191] Researchers have also suggested that another Ca^{2+}/CaN/NFAT signaling pathway plays an important role in bone resorption, formation, and pathophysiology. However, the exact upstream and downstream relationships between this signaling pathway remain unclear and need to be explored further[192] (Fig. 4).

6 Applications of 3D-printed degradable bioceramic scaffolds in clinical settings

6.1 Neurosurgery

In addition to properties such as biocompatibility shared by all 3D-printed scaffolds used in the medical field, site-specific requirements must be addressed for grafts applied to different sites. Scaffolds with multiple functions have been developed for different critical defects, such as maxillofacial, cranial, and long bone. Cranial reconstruction is often used to preserve brain tissue, restore normal contours of the skull, and normal-

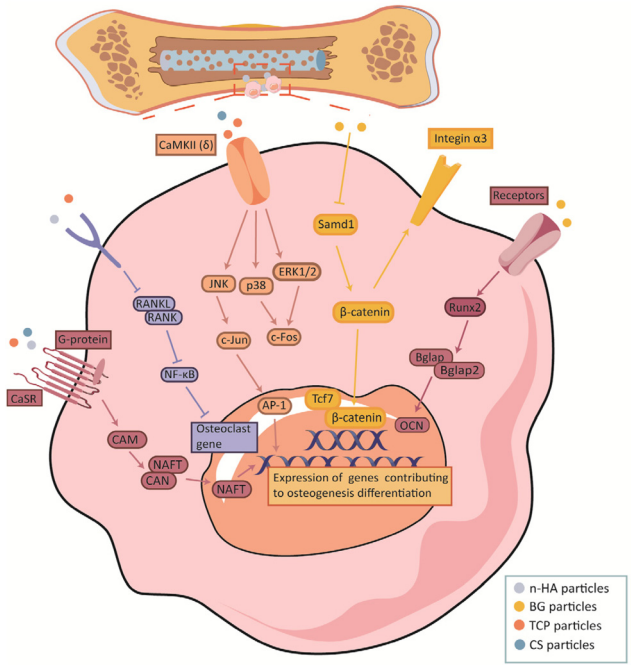

Fig. 4 Illustrations of the other newly found cellular pathways of bio-ceramic.

ize neurological deficits.[193] Bioceramics are attractive bone grafts, and their osteoconductivity, osteoinductivity, and ability to form artifacts in high-field MRI at shallow levels have led to their increased use in cranioplasty.[194–196] 3D-printed bioceramic scaffolds enable precise reconstruction of the skull; thus, the implanted scaffold and defect margins can be well anastomosed during surgery, with satisfactory aesthetic and functional reconstructions and fewer complications observed during the postoperative and follow-up periods.[197]

The use of 3D-printed HA scaffolds in cranial reconstruction has begun to be clinically studied by surgeons.[198,199] In a recent study, the process of repairing the cranium with a 3D-printed scaffold was observed during a 6-month follow-up. Further evidence that the mechanical properties of PCL/β-TCP implants are adequate for cranioplasty is that cranial symmetry was attained immediately following surgery and that neither implant dislocation nor fracture was seen during postoperative follow-up.[200]

6.2 Oral and maxillofacial surgery

Currently, the low degradation rate of bone substitutes and difficulty in matching patient-specific trauma remain clinical and experimental challenges in bone repair.[201] As mentioned above, 3D printing techniques have been used to create patient-specific models for surgeons to visualize bone models and surgical guidelines with precise and predictable results.[202] Simultaneously, the strength of existing bioceramic materials has been proven suitable by researchers for the fabrication of maxillofacial graft scaffolds. Therefore, the development of biodegradable 3D-printed bioceramic materials is an emerging trend in the clinical treatment of oral and maxillofacial bone defects[203] (Table 4).

Although bioceramic scaffolds have shown good properties in repairing maxillofacial bone defects in animal models,[208] few products are currently available in clinical practice. Encouragingly, several combinations of bioceramic and 3D printing technologies appear promising for clinical use, particularly 3D-printed TCP and HA scaffolds that have been successfully tested in humans, suggesting that biodegradable bioceramic scaffolds can be used as reliable bone graft materials to facilitate the bone repair and bone remodeling.[206,209] Researchers have demonstrated a digital approach for creating customized clinical-scale CP scaffolds that can be transplanted into alveolar bone defects using 3D imaging, design, and printing. In addition, a strong foundation for future studies to evaluate personalized medical approaches to treat alveolar bone defects was established.[210] Further studies have demon-

Table 4 3D-printed bio-ceramic materials in oral and maxillofacial surgery

Sites	Number of patients	Materials	Prognosis	Ref.
Mandible	3 patients (1 females and 2 males)	β-TCP	No post operative complications, and no adverse events	204
Maxilla, mandible and frontal bone	20 patients (14 females and 6 males)	α-TCP	One case of infection and three cases of adverse reactions	61
Maxilla and mandible	20 patients (14 females and 6 males)	HA/α-TCP	Four cases of infection	202
Frontal and occipital bone	7 patients (7 males)	PCL/β-TCP	One case of hematoma	200
Cranial bone	25 patients (7 females and 18 males)	HA	No post operative complications, and no adverse events	198
Cranial bone	8 patients (2 females and 6 males)	HA	Two cases of pain and one cases of itching	199
Frontal, temporal and cranial bones	57 patients (2 females and 6 males)	HA	Five cases of infection and two cases of infection	205
Alveolar bone	15 patients (13 females and 2 males)	HA	No post operative complications, and no adverse events	206
Zygomatic bone	10 patients (9 females and 1 males)	CaOSiO2-P2O5-B2O3 glass-ceramics (BGS-7)	No post operative complications, and no adverse events	203
Zygomatic bone	1 patient (male)	BGS-7	No post operative complications, and no adverse events	207

Table 5 3D-printed degradable bio-ceramic scaffold applied to animal bone defect model

Animal	Site	Materials	Fabrication methods	Ref.
New Zealand rabbit	The femur condyle	TCP/BG	DLP	212
	The femoral trochanter	PLA/BG	FDM	215
	The radial diaphysis	TCP	Inkjet printing technology	216
	Mandible	TCP	Inkjet printing technology	217
	Tibia	PTMC/HA	SLA	218
Belgian white rabbit	Cranial bone	PTMC/TCP	SLA	218
Sheep	Tibia	Sr-$Ca_2ZnSi_2O_7$/Al_2O_3	Inkjet printing technology	213
Equine	Tuber coxae bone	MgP/PCL	FDM	219
Beagle dogs	Mandible	HA/TCP	DLP	220
	The dorsal muscles	HA/TCP	DLP	221
Rat	Femoral	TCP	Inkjet printing technology	222
	Femoral	CS	Inkjet printing technology	223
	Cranial bone	HA/TCP	SLA	224
Pig	Tibia	Calcium phosphate	Inkjet printing technology	225
	Mandible	Calcium phosphate	Inkjet printing technology	225

strated promising results in terms of the aesthetics and postoperative prognosis of bioceramic scaffolds.[203,204,206,209] Complications such as infection and hematoma have also been reported in some cases, but optimistic results have been achieved with proper preoperative care and attention.[205] Although researchers have highlighted the bone regeneration potential of biodegradable scaffolds, follow-up studies addressing the clinical sustainability of the scaffold degradation processes are still lacking.

6.3 Orthopedics

The most typical applications of 3D printing technology in bone regeneration of the extremities and joints include bone defects and fracture nonunions. With the development of new equipment and materials, although bioceramic scaffold applications in orthopedic surgery are not yet clinically available, several studies have been conducted to improve the interaction between grafts and their surroundings by tuning the degradability, bioactivity, and other properties of biomaterials.[211] TCP/BG scaffolds with gyroid structures fabricated using DLP effectively induced inward bone growth and fusion in a rabbit femur model.[212] 3D-printed CS composite scaffolds also induced active bone formation and remodeling in a goat tibia critical bone defect model.[213] Numerous preclinical experiments based on animal models have laid the theoretical and practical foundations for the clinical application of bioceramic scaffolds to load-bearing bones. Although only a few studies have reported the use of 3D biodegradable bioceramic scaffolds for upper and lower limb bone repair, they have achieved a low risk of complications and surgical failure in the postoperative period[207,214] (Table 5).

7 Conclusions and perspectives

As discussed above, 3D-printed degradable bioceramic scaffolds have great potential for the treatment of critical bone defects. Bioceramic scaffolds based on advanced 3D printing technologies can be adapted to individual wounds and enable the biomimetic design of bone tissue. In addition, the degradation of the bioceramics effectively promotes cell proliferation and osteogenic differentiation. A series of clinical and preclinical experiments have demonstrated that bioceramics can improve bone repair. However, according to the literature reviewed, the mechanism by which 3D-printed biodegradable bioceramic scaffolds promote bone healing is complex and involves numerous regulatory factors intertwined with signalling networks, and much knowledge remains to be investigated in depth. In addition, current studies about 3D-printed biodegradable bioceramic scaffolds mainly focus on investigating factors and signaling pathways that have been proven to be involved in bone repair. A comprehensive and pioneering understanding of how bioceramic scaffolds promote bone healing remains to be improved. Another fact to consider is that research on biodegradable bioceramic scaffolds is still in the preclinical stage, and there has yet to be a consensus on the printing parameters and feedstocks for using bioceramics for different printing techniques. It is also worth noting that existing clinical reports need more controlled trials and more cases. It is foreseeable that the commercial clinical application of biodegradable bioceramic scaffolds has potential for bone repair, but only after complete testing and clinical trials have demonstrated the safety and efficacy of these scaffolds.

Author contributions

G. Y. and Q. W. conceived the concept of this review. H. L. prepared the original draft. L. Z., Q. Z. and X. W. contributed to the review and editing of the final manuscript.

Conflicts of interest

There are no conflicts to declare.

Acknowledgements

We would like to thank Ning Wang for the revision of our figures. We would like to thank Editage for English language editing.

References

1 E. H. Schemitsch, *J. Orthop. Trauma*, 2017, **31**, S20–S22.
2 F. A. Shah, M. Jolic, C. Micheletti, O. Omar, B. Norlindh, L. Emanuelsson, H. Engqvist, T. Engstrand, A. Palmquist and P. Thomsen, *Bioact. Mater.*, 2023, **19**, 103–114.
3 J. X. Hao, B. S. Bai, Z. Ci, J. C. Tang, G. H. Hu, C. X. Dai, M. Y. Yu, M. Li, W. Zhang, Y. X. Zhang, W. J. Ren, Y. J. Hua and G. D. Zhou, *Bioact. Mater.*, 2022, **14**, 97–109.
4 H. S. Sohn and J. K. Oh, *Biomater. Res.*, 2019, **23**, 9.
5 R. Fairag, D. H. Rosenzweig, J. L. Ramirez-Garcialuna, M. H. Weber and L. Haglund, *ACS Appl. Mater. Interfaces*, 2019, **11**, 15306–15315.
6 P. Baldwin, D. J. Li, D. A. Auston, H. S. Mir, R. S. Yoon and K. J. Koval, *J. Orthop. Trauma*, 2019, **33**, 203–213.
7 S. Tharakan, S. Khondkar and A. Ilyas, *Sensors*, 2021, **21**, 7477.
8 Z. Wang, Y. C. Wang, J. Q. Yan, K. S. Zhang, F. Lin, L. Xiang, L. F. Deng, Z. P. Guan, W. G. Cui and H. B. Zhang, *Adv. Drug Delivery Rev.*, 2021, **174**, 504–534.
9 C. Garot, G. Bettega and C. Picart, *Adv. Funct. Mater.*, 2021, **31**, 2006967.
10 X. Liu, Y. Miao, H. Liang, J. Diao, L. Hao, Z. Shi, N. Zhao and Y. Wang, *Bioact. Mater.*, 2022, **12**, 120–132.
11 R. G. Ribas, V. M. Schatkoski, T. L. D. Montanheiro, B. R. C. de Menezes, C. Stegemann, D. M. G. Leite and G. P. Thim, *Ceram. Int.*, 2019, **45**, 21051–21061.
12 M. A. A. Ansari, A. A. Golebiowska, M. Dash, P. Kumar, P. K. Jain, S. P. Nukavarapu, S. Ramakrishna and H. S. Nanda, *Biomater. Sci.*, 2022, **10**, 2789–2816.
13 M. Vallet-Regi, *Pure Appl. Chem.*, 2019, **91**, 687–706.
14 G. Eugen, M. Claus, S. Anna-Maria, D. Niklas, S. Philipp, E. Andrea, M.-L. Andrea and V. Elke, *Bioact. Mater.*, 2023, **19**, 376–391.
15 A. D. Dalgic, A. Z. Alshemary, A. Tezcaner, D. Keskin and Z. Evis, *J. Biomater. Appl.*, 2018, **32**, 1392–1405.
16 L. Zhang, G. J. Yang, B. N. Johnson and X. F. Jia, *Acta Biomater.*, 2019, **84**, 16–33.
17 L. M. Ulbrich, G. d. S. Balbinot, G. L. Brotto, V. C. B. Leitune, R. M. D. Soares, F. M. Collares and D. Ponzoni, *J. Tissue Eng. Regener. Med.*, 2022, **16**, 267–278.
18 F. Dehghani and N. Annabi, *Curr. Opin. Biotechnol*, 2011, **22**, 661–666.
19 P. K. Juan, F. Y. Fan, W. C. Lin, P. B. Liao, C. F. Huang, Y. K. Shen, M. Ruslin and C. H. Lee, *Polymers*, 2021, **13**, 2718.
20 C. X. Lin, Y. C. Wang, Z. Y. Huang, T. T. Wu, W. K. Xu, W. M. Wu and Z. B. Xu, *Int. J. Bioprint.*, 2021, **7**, 43–64.
21 X. Ye, Y. Zhang, T. Liu, Z. Chen, W. Chen, Z. Wu, Y. Wang, J. Li, C. Li, T. Jiang, Y. Zhang, H. Wu and X. Xu, *Int. J. Biol. Macromol.*, 2022, **209**, 1553–1561.
22 Z. H. Dong, Y. B. Li and Q. Zou, *Appl. Surf. Sci.*, 2009, **255**, 6087–6091.
23 A. T. Xu, C. Zhou, W. T. Qi and F. M. He, *Int. J. Oral Maxillofac. Implants*, 2019, **34**, 434–442.
24 J. B. Vella, R. P. Trombetta, M. D. Hoffman, J. Inzana, H. Awad and D. S. W. Benoit, *J. Biomed. Mater. Res., Part A*, 2018, **106**, 663–667.
25 S. Biscaia, M. V. Branquinho, R. D. Alvites, R. Fonseca, A. C. Sousa, S. S. Pedrosa, A. R. Caseiro, F. Guedes, T. Patrício, T. Viana, A. Mateus, A. C. Maurício and N. Alves, *Int. J. Mol. Sci.*, 2022, **23**, 2318.
26 J. Sonatkar and B. Kandasubramanian, *Eur. Polym. J.*, 2021, **160**, 110801.
27 X. J. Zhang, W. Chang, P. Lee, Y. H. Wang, M. Yang, J. Li, S. G. Kumbar and X. J. Yu, *PLoS One*, 2014, **9**, e85871.
28 X. M. Shi, A. Nommeots-Nomm, N. M. Todd, A. Devlin-Mullin, H. Geng, P. D. Lee, C. A. Mitchell and J. R. Jones, *Appl. Mater. Today*, 2020, **20**, 100770.
29 T. Johnson, R. Bahrampourian, A. Patel and K. Mequanint, *Bio-Med. Mater. Eng.*, 2010, **20**, 107–118.
30 M. Xu, H. Li, D. Zhai, J. Chang, S. Chen and C. Wu, *J. Mater. Chem. B*, 2015, **3**, 3799–3809.
31 X. M. Dong, A. Heidari, A. Mansouri, W. S. Hao, M. Dehghani, S. Saber-Samandari, D. Toghraie and A. Khandan, *J. Mech. Behav. Biomed. Mater.*, 2021, **121**, 104643.
32 J. Z. Yang, X. Z. Hu, R. Sultana, R. E. Day and P. Ichim, *Biomed. Mater.*, 2015, **10**, 045006.
33 M. Dehurtevent, L. Robberecht, J.-C. Hornez, A. Thuault, E. Deveaux and P. Behin, *Dent. Mater.*, 2017, **33**, 477–485.
34 L. Breideband, K. N. Waechtershaeuser, L. Hafa, K. Wieland, A. S. Frangakis, E. H. K. Stelzer and F. Pampaloni, *Adv. Mater. Technol.*, 2022, **7**, 2200029.
35 A. Smirnov, S. Chugunov, A. Kholodkova, M. Isachenkov, A. Tikhonov, O. Dubinin and I. Shishkovsky, *Materials*, 2022, **15**, 960.
36 O. Guillaume, M. A. Geven, C. M. Sprecher, V. A. Stadelmann, D. W. Grijpma, T. T. Tang, L. Qin, Y. Lai, M. Alini, J. D. de Bruijn, H. Yuan, R. G. Richards and D. Eglin, *Acta Biomater.*, 2017, **54**, 386–398.
37 S. Derakhshanfar, R. Mbeleck, K. Xu, X. Zhang, W. Zhong and M. Xing, *Bioact. Mater.*, 2018, **3**, 144–156.
38 C. Yu, J. Schimelman, P. Wang, K. L. Miller, X. Ma, S. You, J. Guan, B. Sun, W. Zhu and S. Chen, *Chem. Rev.*, 2020, **120**, 10748–10796.
39 S. B. Hua, X. Yuan, J. M. Wu, J. Su, L. J. Cheng, W. Zheng, M. Z. Pan, J. Xiao and Y. S. Shi, *Ceram. Int.*, 2022, **48**, 3020–3029.
40 A. Bagheri and J. Y. Jin, *ACS Appl. Polym. Mater.*, 2019, **1**, 593–611.
41 S. L. Sing, W. Y. Yeong, F. E. Wiria, B. Y. Tay, Z. Q. Zhao, L. Zhao, Z. L. Tian and S. F. Yang, *Rapid Prototyp J.*, 2017, **23**, 611–623.

42 Y. Du, H. Liu, Q. Yang, S. Wang, J. Wang, J. Ma, I. Noh, A. G. Mikos and S. Zhang, *Biomaterials*, 2017, **137**, 37–48.
43 F. Lupone, E. Padovano, M. Pietroluongo, S. Giudice, O. Ostrovskaya and C. Badini, *eXPRESS Polym. Lett.*, 2021, **15**, 177–192.
44 J. Shen, B. Chen, X. Zhai, W. Qiao, S. Wu, X. Liu, Y. Zhao, C. Ruan, H. Pan, P. K. Chu, K. M. C. Cheung and K. W. K. Yeung, *Bioact. Mater.*, 2021, **6**, 503–519.
45 B. C. Lei, X. B. Gao, R. Zhang, X. Yi and Q. Zhou, *Mater. Des.*, 2022, **215**, 110477.
46 Q. F. Wang, W. J. Ye, Z. Y. Ma, W. J. Xie, L. N. Zhong, Y. Wang and Q. Rong, *Mater. Sci. Eng., C*, 2021, **127**, 112197.
47 H. Wang, Z. W. Deng, J. Chen, X. Qi, L. B. Pang, B. C. Lin, Y. T. Y. Adib, N. Miao, D. P. Wang, Y. D. Zhang, J. S. Li and X. Q. Zeng, *Int. J. Biol. Sci.*, 2020, **16**, 1821–1832.
48 C. L. Wang, C. Y. Meng, Z. Zhang and Q. S. Zhu, *Ceram. Int.*, 2022, **48**, 7491–7499.
49 C. M. Gonzalez-Henriquez, M. A. Sarabia-Vallejos and J. Rodriguez-Hernandez, *Prog. Polym. Sci.*, 2019, **94**, 57–116.
50 S. Singh, S. Ramakrishna and R. Singh, *J. Manuf. Process*, 2017, **25**, 185–200.
51 W. Wang, B. Zhang, M. Li, J. Li, C. Zhang, Y. Han, L. Wang, K. Wang, C. Zhou, L. Liu, Y. Fan and X. Zhang, *Composites, Part B*, 2021, **224**, 109192.
52 L. Zhao, X. Wang, H. Xiong, K. Zhou and D. Zhang, *J. Eur. Ceram. Soc.*, 2021, **41**, 5066–5074.
53 J. H. Park, J. Jang, J. S. Lee and D. W. Cho, *Tissue Eng. Regener. Med.*, 2016, **13**, 612–621.
54 D. Graf, A. Qazzazie and T. Hanemann, *Materials*, 2020, **13**, 2587.
55 Z. J. Peng, X. D. Luo, Z. P. Xie, D. An and M. M. Yang, *Ceram. Int.*, 2018, **44**, 16766–16772.
56 X. Wang, M. Zhang, L. Zhang, J. Xu, X. Xiao and X. Zhang, *Mater. Today Commun.*, 2022, **31**, 103263.
57 G. F. Gao and X. F. Cui, *Biotechnol. Lett.*, 2016, **38**, 203–211.
58 M. A. Shah, D. G. Lee, B. Y. Lee and S. Hur, *IEEE Access*, 2021, **9**, 140079–140102.
59 J. Chang, M. Chi, T. Shen and Z. Liang, *J. Adhes. Sci. Technol.*, 2020, **34**, 1128–1143.
60 H. C. Ji, X. J. Zhang, W. C. Pei, Y. G. Li, L. Zheng, X. M. Ye and Y. H. Lu, *Cailiao Gongcheng*, 2018, **46**, 19–28.
61 H. Saijo, Y. Fujihara, Y. Kanno, K. Hoshi, A. Hikita, U.-i. Chung and T. Takato, *Regen. Ther.*, 2016, **5**, 72–78.
62 D. Dong, H. J. Su, X. Li, G. R. Fan, D. Zhao, Z. L. Shen, Y. Liu, Y. N. Guo, C. B. Yang, L. Liu and H. Z. Fu, *J. Manuf. Process*, 2022, **81**, 433–443.
63 A. J. Guerra, H. Lara-Padilla, M. L. Becker, C. A. Rodriguez and D. Dean, *Curr. Drug Targets*, 2019, **20**, 823–838.
64 Y. Luo, G. Le Fer, D. Dean and M. L. Becker, *Biomacromolecules*, 2019, **20**, 1699–1708.
65 A. Kafle, E. Luis, R. Silwal, H. M. Pan, P. L. Shrestha and A. K. Bastola, *Polymers*, 2021, **13**, 3101.
66 I. K. Cingesar, M. P. Markovic and D. Vrsaljko, *Addit. Manuf.*, 2022, **55**, 102813.
67 A. J. Guerra, J. Lammel-Lindemann, A. Katko, A. Kleinfehn, C. A. Rodriguez, L. H. Catalani, M. L. Becker, J. Ciurana and D. Dean, *Acta Biomater.*, 2019, **97**, 154–161.
68 T. Zandrini, S. Florczak, R. Levato and A. Ovsianikov, *Trends Biotechnol.*, 2023, **41**, 604–614.
69 Q. Lian, F. Yang, H. Xin and D. Li, *Ceram. Int.*, 2017, **43**, 14956–14961.
70 Y. Tian, H. Ma, X. Yu, B. Feng, Z. Yang, W. Zhang and C. Wu, *Biomed. Mater.*, 2023, **18**, 034102.
71 C. J. Shuai, P. Feng, C. D. Cao and S. P. Peng, *Biotechnol. Bioprocess Eng.*, 2013, **18**, 520–527.
72 A. Alahnoori, M. Badrossamay and E. Foroozmehr, *Mater. Chem. Phys.*, 2023, **296**, 127316.
73 C. J. Shuai, H. Sun, C. D. Gao, P. Feng, W. Guo, W. J. Yang, H. Xu, Q. Li, Y. W. Yang and S. P. Peng, *Appl. Surf. Sci.*, 2018, **455**, 1150–1160.
74 W. Z. Wang, B. Q. Zhang, L. H. Zhao, M. X. Li, Y. L. Han, L. Wang, Z. D. Zhang, J. Li, C. C. Zhou and L. Liu, *Nanotechnol. Rev.*, 2021, **10**, 1359–1373.
75 R. Han, F. Buchanan, L. Ford, M. Julius and P. J. Walsh, *Mater. Sci. Eng., C*, 2021, **120**, 111755.
76 Q. Fu, E. Saiz and A. P. Tomsia, *Acta Biomater.*, 2011, **7**, 3547–3554.
77 D. Mondal and T. L. Willett, *J. Mech. Behav. Biomed. Mater.*, 2020, **104**, 103653.
78 J. J. Diao, J. OuYang, T. Deng, X. Liu, Y. T. Feng, N. R. Zhao, C. B. Mao and Y. J. Wang, *Adv. Healthcare Mater.*, 2018, **7**, e1800441.
79 M. Ramu, M. Ananthasubramanian, T. Kumaresan, R. Gandhinathan and S. Jothi, *Bio-Med. Mater. Eng.*, 2018, **29**, 739–755.
80 H. Schappo, G. V. Salmoria, A. Magnaudeix, A. Dumur, E. Renaudie, K. Giry, C. Damia and D. Hotza, *Powder Technol.*, 2022, **412**, 117966.
81 S. F. S. Shirazi, S. Gharehkhani, M. Mehrali, H. Yarmand, H. S. C. Metselaar, N. A. Kadri and N. A. A. Osman, *Sci. Technol. Adv. Mater.*, 2015, **16**, 033502.
82 N. Kamboj, A. Ressler and I. Hussainova, *Materials*, 2021, **14**, 5338.
83 S. Chaudhary, S. K. Avinashi, J. T. D. Rao and C. Gautam, *ACS Biomater. Sci. Eng.*, 2023, **9**, 3987–4019.
84 K. Senthilkumaran, P. M. Pandey and P. V. M. Rao, *Mater. Des.*, 2009, **30**, 2946–2954.
85 H. Park, J. Ryu, S. Jung, H. Park, H. Oh and M. Kook, *Materials*, 2022, **15**, 827.
86 B. Q. Zhang, L. Wang, P. Song, X. Pei, H. Sun, L. A. Wu, C. C. Zhou, K. F. Wang, Y. J. Fan and X. D. Zhang, *Mater. Des.*, 2021, **201**, 109490.
87 S. Garzon-Hernandez, A. Arias and D. Garcia-Gonzalez, *Composites, Part B*, 2020, **201**, 108373.
88 B. Derby, *J. Eur. Ceram. Soc.*, 2011, **31**, 2543–2550.
89 C. F. Marques, G. S. Diogo, S. Pina, J. M. Oliveira, T. H. Silva and R. L. Reis, *J. Mater. Sci.: Mater. Med.*, 2019, **30**, 32.
90 K. B. Devi, B. Tripathy, P. N. Kumta, S. K. Nandi and M. Roy, *ACS Biomater. Sci. Eng.*, 2018, **4**, 2126–2133.

91 M. S. Attia, H. M. Mohammed, M. G. Attia, M. A. Hamid and E. A. Shoeriabah, *J. Periodontol.*, 2019, **90**, 281–287.
92 Z. B. Liu, H. X. Liang, T. S. Shi, D. Q. Xie, R. Y. Chen, X. Han, L. D. Shen, C. J. Wang and Z. J. Tian, *Ceram. Int.*, 2019, **45**, 11079–11086.
93 H. Y. Chang, W. H. Tuan and P. L. Lai, *Mater. Sci. Eng., C*, 2021, **118**, 111421.
94 H. L. Li, L. L. Li, Y. Q. He, W. Mao, H. F. Ni, A. L. Yang, F. Z. Lyu and Y. H. Dong, *Stem Cells Int.*, 2021, **2021**, 8359582.
95 Y. R. Cai, Y. K. Liu, W. Q. Yan, Q. H. Hu, J. H. Tao, M. Zhang, Z. L. Shi and R. K. Tang, *J. Mater. Chem.*, 2007, **17**, 3780–3787.
96 G. Balasundaram, M. Sato and T. J. Webster, *Biomaterials*, 2006, **27**, 2798–2805.
97 X. B. Chen, C. X. Gao, J. W. Jiang, Y. P. Wu, P. Z. Zhu and G. Chen, *Biomed. Mater.*, 2019, **14**, 065003.
98 Z. Geng, X. P. Li, L. L. Ji, Z. Y. Li, S. L. Zhu, Z. D. Cui, J. Wang, J. Y. Cui, X. J. Yang and C. S. Liu, *J. Mater. Sci. Technol.*, 2021, **79**, 35–45.
99 O. Demir-Oguz, A. R. Boccaccini and D. Loca, *Bioact. Mater.*, 2023, **19**, 217–236.
100 S. H. Rao, B. Harini, R. P. K. Shadamarshan, K. Balagangadharan and N. Selvamurugan, *Int. J. Biol. Macromol.*, 2018, **110**, 88–96.
101 Z. Fan, J. Wang, F. Liu, Y. Nie, L. Ren and B. Liu, *Colloids Surf., B*, 2016, **145**, 438–446.
102 H. Jodati, B. Yilmaz and Z. Evis, *Ceram. Int.*, 2020, **46**, 15725–15739.
103 E. B. Montufar, K. Slámečka, M. Casas-Luna, P. Skalka, E. Ramírez-Cedillo, M. Zborčák, J. Kaiser and L. Čelko, *J. Eur. Ceram. Soc.*, 2020, **40**, 4923–4931.
104 F. P. He, X. Y. Yuan, T. L. Lu, Y. Wang, S. H. Feng, X. T. Shi, L. Wang, J. D. Ye and H. Yang, *J. Mater. Chem. B*, 2022, **10**, 4040–4047.
105 Y. X. Li, W. Liao, T. Taghvaee, C. L. Wu, H. Y. Ma and N. Leventis, *Mater. Lett.*, 2019, **237**, 274–277.
106 F. S. Shirazi, M. Mehrali, A. A. Oshkour, H. S. Metselaar, N. A. Kadri and N. A. A. Osman, *J. Mech. Behav. Biomed. Mater.*, 2014, **30**, 168–175.
107 P. Srinath, P. A. Azeem and K. V. Reddy, *Int. J. Appl. Ceram. Technol.*, 2020, **17**, 2450–2464.
108 J. Bejarano, A. R. Boccaccini, C. Covarrubias and H. Palza, *Materials*, 2020, **13**, 2908.
109 J. R. Jones, *Acta Biomater.*, 2013, **9**, 4457–4486.
110 C. Zhao, W. Liu, M. Zhu, C. Wu and Y. Zhu, *Bioact. Mater.*, 2022, **18**, 383–398.
111 K. C. R. Kolan, Y.-W. Huang, J. A. Semon and M. C. Leu, *Int. J. Bioprint.*, 2020, **6**, 274.
112 J. Zhang, W. Wei, L. L. Yang, Y. K. Pan, X. H. Wang, T. L. Wang, S. C. Tang, Y. Yao, H. Hong and J. Wei, *Colloids Surf., B*, 2018, **164**, 347–357.
113 G. S. Polymeris, V. Giannoulatou, A. Kyriakidou, I. K. Sfampa, G. S. Theodorou, E. Sahiner, N. Meric, G. Kitis and K. M. Paraskevopoulos, *Mater. Sci. Eng., C*, 2017, **70**, 673–680.
114 G. Gomez and L. E. Westerlund, *J Spine Surg.*, 2021, **7**, 124–131.
115 K. E. Kojima, E. S. F. B. de Andrade, M. C. Leonhardt, V. C. de Carvalho, P. R. D. de Oliveira, A. Lima, P. R. D. Reis and J. D. S. Silva, *Injury*, 2021, **52**(Suppl 3), S23–S28.
116 D. G. Armstrong, D. P. Orgill, R. D. Galiano, P. M. Glat, L. A. DiDomenico, M. J. Carter and C. M. Zelen, *Int Wound J.*, 2022, **19**, 791–801.
117 A. C. Profeta and G. M. Prucher, *Open Dent. J.*, 2017, **11**, 164–170.
118 R. S. Pereira, J. D. Menezes, J. P. Bonardi, G. L. Griza, R. Okamoto and E. Hochuli-Vieira, *Int. J. Oral Maxillofac. Surg.*, 2018, **47**, 665–671.
119 P. Stoor, S. Apajalahti and R. Kontio, *J. Craniofac. Surg.*, 2017, **28**, 1197–1205.
120 H. Sun, C. Hu, C. C. Zhou, L. N. Wu, J. X. Sun, X. D. Zhou, F. Xing, C. Long, Q. Q. Kong, J. Liang, Y. Fan and X. Zhang, *Mater. Des.*, 2020, **189**, 108540.
121 I. Uiiah, L. Cao, W. Cui, Q. Xu, R. Yang, K. L. Tang and X. Zhang, *J. Mater. Sci. Technol.*, 2021, **88**, 99–108.
122 A. Barba, Y. Maazouz, A. Diez-Escudero, K. Rappe, M. Espanol, E. B. Montufar, C. Ohman-Magi, C. Persson, P. Fontecha, M. C. Manzanares, J. Franch and M. P. Ginebra, *Acta Biomater.*, 2018, **79**, 135–147.
123 C. Wang, J. H. Lai, K. Li, S. K. Zhu, B. H. Lu, J. Liu, Y. J. Tang and Y. Wei, *Bioact. Mater.*, 2021, **6**, 137–145.
124 M. Nabiyouni, T. Bruckner, H. Zhou, U. Gbureck and S. B. Bhaduri, *Acta Biomater.*, 2018, **66**, 23–43.
125 A. Zheng, L. Y. Cao, Y. Liu, J. N. Wu, D. L. Zeng, L. W. Hu, X. K. Zhang and X. Q. Jiang, *Carbohydr. Polym.*, 2018, **199**, 244–255.
126 H. Zhang, C. Jiao, Z. He, M. Ge, Z. Tian, C. Wang, Z. Wei, L. Shen and H. Liang, *Ceram. Interfaces*, 2021, **47**, 27032–27041.
127 C. Wang, Y. Xue, K. Lin, J. Lu, J. Chang and J. Sun, *Acta Biomater.*, 2012, **8**, 350–360.
128 H. F. Shao, X. R. Ke, A. Liu, M. Sun, Y. He, X. Y. Yang, J. Z. Fu, Y. M. Liu, L. Zhang, G. J. Yang, S. Z. Xu and Z. R. Gou, *Biofabrication*, 2017, **9**, 025003.
129 Z. J. He, C. Jiao, H. X. Zhang, D. Q. Xie, M. X. Ge, Y. W. Yang, G. F. Wu, H. X. Liang, L. D. Shen and C. J. Wang, *Ceram. Interfaces*, 2022, **48**, 25923–25932.
130 Z. Chen, T. Klein, R. Z. Murray, R. Crawford, J. Chang, C. Wu and Y. Xiao, *Mater. Today*, 2016, **19**, 304–321.
131 A. Schindeler, M. M. McDonald, P. Bokko and D. G. Little, *Semin. Cell Dev. Biol.*, 2008, **19**, 459–466.
132 S. Franz, S. Rammelt, D. Scharnweber and J. C. Simon, *Biomaterials*, 2011, **32**, 6692–6709.
133 A. Shapouri-Moghaddam, S. Mohammadian, H. Vazini, M. Taghadosi, S.-A. Esmaeili, F. Mardani, B. Seifi, A. Mohammadi, J. T. Afshari and A. Sahebkar, *J. Cell. Physiol.*, 2018, **233**, 6425–6440.
134 K. Hu and B. R. Olsen, *Bone*, 2016, **91**, 30–38.
135 H. Newman, Y. V. Shih and S. Varghese, *Biomaterials*, 2021, **277**, 121114.

136 K. Zheng, W. Niu, B. Lei and A. R. Boccaccini, *Acta Biomater.*, 2021, **133**, 168–186.
137 X. Chen, M. Wang, F. Chen, J. Wang, X. Li, J. Liang, Y. Fan, Y. Xiao and X. Zhang, *Acta Biomater.*, 2020, **103**, 318–332.
138 W. Xie, X. Fu, F. Tang, Y. Mo, J. Cheng, H. Wang and X. Chen, *J. Mater. Chem. B*, 2019, **7**, 940–952.
139 P. Guihard, Y. Danger, B. Brounais, E. David, R. Brion, J. Delecrin, C. Richards, S. Chevalier, F. Redini, D. Heymann, H. Gascan and F. Blanchard, *Bone*, 2012, **50**, S83–S83.
140 P. L. Graney, S. Ben-Shaul, S. Landau, A. Bajpai, B. Singh, J. Eager, A. Cohen, S. Levenberg and K. L. Spiller, *Sci. Adv.*, 2020, **6**, eaay6391.
141 L. Y. Lu, F. Loi, K. Nathan, T.-h. Lin, J. Pajarinen, E. Gibon, A. Nabeshima, L. Cordova, E. Jamsen, Z. Yao and S. B. Goodman, *J. Orthop. Res.*, 2017, **35**, 2378–2385.
142 T. A. Einhorn and L. C. Gerstenfeld, *Nat. Rev. Rheumatol.*, 2015, **11**, 45–54.
143 S. D. Dutta, T. V. Patil, K. Ganguly, A. Randhawa and K.-T. Lim, *Bioact. Mater.*, 2023, **28**, 284–310.
144 S. Hoshikawa, K. Shimizu, A. Watahiki, M. Chiba, K. Saito, W. Wei, S. Fukumoto and H. Inuzuka, *FASEB J.*, 2020, **34**, 14930–14945.
145 K. Hu and B. R. Olsen, *J. Clin. Invest.*, 2016, **126**, 509–526.
146 Q.-L. Ma, L. Fang, N. Jiang, L. Zhang, Y. Wang, Y.-M. Zhang and L.-H. Chen, *Biomaterials*, 2018, **154**, 234–247.
147 T. Li, M. Peng, Z. Yang, X. Zhou, Y. Deng, C. Jiang, M. Xiao and J. Wang, *Acta Biomater.*, 2018, **71**, 96–107.
148 H. Li, W. Wang and J. Chang, *Regener. Biomater.*, 2021, **8**, rbab056.
149 B. Liang, H. Wang, D. Wu and Z. Wang, *J. Leukocyte Biol.*, 2021, **110**, 433–447.
150 W. Qiao, H. Xie, J. Fang, J. Shen, W. Li, D. Shen, J. Wu, S. Wu, X. Liu, Y. Zheng, K. M. C. Cheung and K. W. K. Yeung, *Biomaterials*, 2021, **276**, 121038.
151 K. Arvidson, B. M. Abdallah, L. A. Applegate, N. Baldini, E. Cenni, E. Gomez-Barrena, D. Granchi, M. Kassem, Y. T. Konttinen, K. Mustafa, D. P. Pioletti, T. Sillat and A. Finne-Wistrand, *J. Cell. Mol. Med.*, 2011, **15**, 718–746.
152 L. Voisin, M. K. Saba-El-Leil, C. Julien, C. Fremin and S. Meloche, *Mol. Cell. Biol.*, 2010, **30**, 2918–2932.
153 M. Majidinia, A. Sadeghpour and B. Yousefi, *J. Cell. Physiol.*, 2018, **233**, 2937–2948.
154 W. Zhang and H. T. Liu, *Cell Res.*, 2002, **12**, 9–18.
155 W. Hatakeyama, M. Taira, N. Chosa, H. Kihara, A. Ishisaki and H. Kondo, *Int. J. Mol. Med.*, 2013, **32**, 1255–1261.
156 Y. Huang, G. Zhou, L. S. Zheng, H. F. Liu, X. F. Niu and Y. B. Fan, *Nanoscale*, 2012, **4**, 2484–2490.
157 S. W. Ha, J. Park, M. M. Habib and G. R. Beck, *ACS Appl. Mater. Interfaces*, 2017, **9**, 39185–39196.
158 N. Wang, S. Yang, H. X. Shi, Y. P. Song, H. Sun, Q. Wang, L. L. Tan and S. Guo, *J. Magnesium Alloys*, 2022, **10**, 3327–3353.
159 S. H. Lin, G. Z. Yang, F. Jiang, M. L. Zhou, S. Yin, Y. M. Tang, T. T. Tang, Z. Y. Zhang, W. J. Zhang and X. Q. Jiang, *Adv. Sci.*, 2019, **6**, 1900209.
160 Z. T. Wang, Q. Liu, C. C. Liu, W. Tan, M. Y. Tang, X. H. Zhou, T. S. Sun and Y. W. Deng, *J. Cell. Physiol.*, 2020, **235**, 5182–5191.
161 M. Li, P. He, Y. H. Wu, Y. Zhang, H. Xia, Y. F. Zheng and Y. Han, *Sci. Rep.*, 2016, **6**, 32323.
162 M. Y. Shie and S. J. Ding, *Biomaterials*, 2013, **34**, 6589–6606.
163 C. H. Liu, C. J. Hung, T. H. Huang, C. C. Lin, C. T. Kao and M. Y. Shie, *Mater. Sci. Eng., C*, 2014, **43**, 359–366.
164 B. C. Wu, C. T. Kao, T. H. Huang, C. J. Hung, M. Y. Shie and H. Y. Chung, *J. Endod.*, 2014, **40**, 1105–1111.
165 E. Rathinam, S. Rajasekharan, R. T. Chitturi, H. Declercq, L. Martens and P. De Coster, *J. Endod.*, 2016, **42**, 1713–1725.
166 S. X. Lai, L. J. Chen, W. Cao, S. M. Cui, X. Y. Li, W. C. Zhong, M. Y. Ma and Q. B. Zhang, *Mediators Inflammation*, 2018, **2018**, 8167932.
167 G. Luther, E. R. Wagner, G. H. Zhu, Q. Kang, Q. Luo, J. Lamplot, Y. Bi, X. J. Luo, J. Y. Luo, C. Teven, Q. Shi, S. H. Kim, J. L. Gao, E. Y. Huang, K. Yang, R. Rames, X. Liu, M. Li, N. Hu, H. Liu, Y. X. Su, L. Chen, B. C. He, G. W. Zuo, Z. L. Deng, R. R. Reid, H. H. Luu, R. C. Haydon and T. C. He, *Curr. Gene Ther.*, 2011, **11**, 229–240.
168 L. F. Hu, C. Yin, F. Zhao, A. Ali, J. H. Ma and A. R. Qian, *Int. J. Mol. Sci.*, 2018, **19**, 360.
169 C. H. Heldin, M. Landstrom and A. Moustakas, *Curr. Opin. Cell Biol.*, 2009, **21**, 166–176.
170 S. Vermeulen, Z. T. Birgani and P. Habibovic, *Biomaterials*, 2022, **283**, 121431.
171 M. Bruderer, R. G. Richards, M. Alini and M. J. Stoddart, *Eur. Cells Mater.*, 2014, **28**, 269–286.
172 Z. R. Tang, Z. Wang, F. Z. Qing, Y. L. Ni, Y. J. Fan, Y. F. Tan and X. D. Zhang, *J. Biomed. Mater. Res., Part A*, 2015, **103**, 1001–1010.
173 J. Wang, M. L. Wang, F. Y. Chen, Y. H. Wei, X. N. Chen, Y. Zhou, X. Yang, X. D. Zhu, C. Q. Tu and X. D. Zhang, *Int. J. Nanomed.*, 2019, **14**, 7987–8000.
174 Z. T. Chen, C. T. Wu, W. Y. Gu, T. Klein, R. Crawford and Y. Xiao, *Biomaterials*, 2014, **35**, 1507–1518.
175 D. Zhai, M. C. Xu, L. Q. Liu, J. Chang and C. T. Wu, *J. Mater. Chem. B*, 2017, **5**, 7297–7306.
176 F. Han, T. Li, M. M. Li, B. J. Zhang, Y. F. Wang, Y. F. Zhu and C. T. Wu, *Bioact. Mater.*, 2023, **20**, 29–40.
177 C. Y. Janda, D. Waghray, A. M. Levin, C. Thomas and K. C. Garcia, *Science*, 2012, **337**, 59–64.
178 L. Mao, J. Liu, J. Zhao, J. Chang, L. Xia, L. Jiang, X. Wang, K. Lin and B. Fang, *Int. J. Nanomed.*, 2015, **10**, 7031–7044.
179 M. T. Zheng, M. J. Weng, X. Y. Zhang, R. M. Li, Q. Tong and Z. Q. Chen, *Biomed. Mater.*, 2021, **16**, 025005.
180 R. L. Wang, L. J. Chen and L. Q. Shao, *J. Nanobiotechnol.*, 2020, **18**, 119.
181 X. Cui, Y. Zhang, J. Wang, C. Huang, Y. Wang, H. Yang, W. Liu, T. Wang, D. Wang, G. Wang, C. Ruan, D. Chen, W. W. Lu, W. Huang, M. N. Rahaman and H. Pan, *Bioact. Mater.*, 2020, **5**, 334–347.
182 C. C. Yin, X. S. Jia, Q. Zhao, Z. F. Zhao, J. Y. Wang, Y. F. Zhang, Z. Li, H. C. Sun and Z. B. Li, *Mater. Sci. Eng., C*, 2020, **110**, 110671.

183 Y. Chen, L. Chen, Y. T. Wang, K. L. Lin and J. Q. Liu, *Composites, Part B*, 2022, **230**, 109550.
184 F. J. Zhao, Z. Yang, H. C. Xiong, Y. Yan, X. F. Chen and L. Q. Shao, *Bioact. Mater.*, 2023, **22**, 201–210.
185 P. Feng, P. Wu, C. Gao, Y. Yang, W. Guo, W. Yang and C. Shuai, *Adv. Sci.*, 2018, **5**, 1700817.
186 M. Bohner and R. J. Miron, *Mater. Today*, 2019, **22**, 132–141.
187 H. P. Lu, Y. H. Zhou, Y. P. Ma, L. Xiao, W. J. Ji, Y. Zhang and X. Wang, *Front. Mater.*, 2021, **8**, 698915.
188 D. Z. Lu, W. Dong, X. J. Feng, H. Chen, J. J. Liu, H. Wang, L. Y. Zang and M. C. Qi, *Mol. Cell. Endocrinol.*, 2020, **508**, 110791.
189 S. Kanaya, B. L. Xiao, Y. Sakisaka, M. Suto, K. Maruyama, M. Saito and E. Nemoto, *J. Appl. Oral Sci.*, 2018, **26**, e20170231.
190 A. De, *Acta Biochim. Biophys. Sin.*, 2011, **43**, 745–756.
191 X. G. Wang, Y. M. Yu, L. L. Ji, Z. Geng, J. Wang and C. S. Liu, *Bioact. Mater.*, 2021, **6**, 4517–4530.
192 R. Y. Ren, J. C. Guo, Y. M. F. Chen, Y. Y. Zhang, L. X. Chen and W. Xiong, *Cell Proliferation*, 2021, **54**, e13122.
193 J. C. Lee and E. J. Volpicelli, *Adv. Healthcare Mater.*, 2017, **6**, 1700232.
194 M. Maroulakos, G. Kamperos, L. Tayebi, D. Halazonetis and Y. J. Ren, *J. Dent.*, 2019, **80**, 1–14.
195 H. Matsuura, T. Inoue, H. Konno, M. Sasaki, K. Ogasawara and A. Ogawa, *J. Neurosurg.*, 2002, **97**, 1472–1475.
196 V. Siracusa, G. Maimone and V. Antonelli, *Polymers*, 2021, **13**, 1452.
197 J. Brie, T. Chartier, C. Chaput, C. Delage, B. Pradeau, F. Caire, M. P. Boncoeur and J. J. Moreau, *J Craniomaxillofac. Surg.*, 2013, **41**, 403–407.
198 P. C. Whitfield, *Acta Neurochirurgica*, 2007, **149**, 170–170.
199 J. Brie, T. Chartier, C. Chaput, C. Delage, B. Pradeau, F. Caire, M. P. Boncoeur and J. J. Moreau, *J Craniomaxillofac. Surg.*, 2013, **41**, 403–407.
200 H. Park, J. W. Choi and W. S. Jeong, *J. Craniofac. Surg.*, 2022, **33**, 1394–1399.
201 A. Hikita, U. I. Chung, K. Hoshi and T. Takato, *Tissue Eng., Part A*, 2017, **23**, 515–521.
202 Y. Kanno, T. Nakatsuka, H. Saijo, Y. Fujihara, H. Atsuhiko, U. I. Chung, T. Takato and K. Hoshi, *Regen. Ther.*, 2016, **5**, 1–8.
203 U. L. Lee, J. Y. Lim, S. N. Park, B. H. Choi, H. Kang and W. C. Choi, *Materials*, 2020, **13**, 4515.
204 J. Wolff, G. K. Sandor, A. Miettinen, V. J. Tuovinen, B. Mannerstrom, M. Patrikoski and S. Miettinen, *Ann. Maxillofac. Surg.*, 2013, **3**, 114–125.
205 H. B. Chen, J. M. Sun and J. C. Wang, *J. Craniofac. Surg.*, 2018, **29**, 618–621.
206 P. Kijartorn, J. Wongpairojpanich, F. Thammarakcharoen, J. Suwanprateeb and B. Buranawat, *J. Dent. Sci.*, 2022, **17**, 194–203.
207 H. Jo and U. L. Lee, *J. Craniofac. Surg.*, 2022, **33**, E521–E523.
208 F. F. Xu, H. Ren, M. J. Zheng, X. X. Shao, T. Q. Dai, Y. L. Wu, L. Tian, Y. Liu, B. Liu, J. Gunster, Y. X. Liu and Y. P. Liu, *J. Mech. Behav. Biomed. Mater.*, 2020, **103**, 103532.
209 C. Mangano, A. Giuliani, I. De Tullio, M. Raspanti, A. Piattelli and G. Iezzi, *Front. Bioeng. Biotechnol.*, 2021, **9**, 614325.
210 M. Anderson, N. Dubey, K. Bogie, C. Cao, J. Y. Li, J. Lerchbacker, G. Mendonca, F. Kauffmann, M. C. Bottino and D. Kaigler, *Dent. Mater.*, 2022, **38**, 529–539.
211 M. Navarro, A. Michiardi, O. Castano and J. A. Planell, *J. R. Soc., Interface*, 2008, **5**, 1137–1158.
212 H. Zhu, M. Li, X. L. Huang, D. H. Qi, L. P. Nogueira, X. Yuan, W. B. Liu, Z. H. Lei, J. W. Jiang, H. L. Dai and J. Xiao, *Appl. Mater. Today*, 2021, **25**, 101166.
213 J. J. Li, C. R. Dunstan, A. Entezari, Q. Li, R. Steck, S. Saifzadeh, A. Sadeghpour, J. R. Field, A. Akey, M. Vielreicher, O. Friedrich, S. Roohani-Esfahani and H. Zreiqat, *Adv. Healthcare Mater.*, 2019, **8**, e1801298.
214 Y. J. Lu, G. J. Chen, Z. Y. Long, M. H. Li, C. L. Ji, F. W. Wang, H. Z. Li, J. X. Lu, Z. Wang and J. Li, *J. Bone Oncol.*, 2019, **16**, 100220.
215 Y. R. Ding, X. L. Liu, J. Zhang, Z. C. Lv, X. C. Meng, Z. G. Yuan, T. Long and Y. Wang, *Front. Bioeng. Biotechnol.*, 2022, **10**, 947521.
216 L. Witek, A. M. Alifarag, N. Tovar, C. D. Lopez, B. N. Cronstein, E. D. Rodriguez and P. G. Coelho, *J. Orthop. Res.*, 2019, **37**, 2499–2507.
217 C. D. Lopez, J. R. Diaz-Siso, L. Witek, J. M. Bekisz, B. N. Cronstein, A. Torroni, R. L. Flores, E. D. Rodriguez and P. G. Coelho, *J. Surg. Res.*, 2018, **223**, 115–122.
218 A. K. Teotia, K. Dienel, I. Qayoom, B. van Bochove, S. Gupta, J. Partanen, J. Seppala and A. Kumar, *ACS Appl. Mater. Interfaces*, 2020, **12**, 48340–48356.
219 N. Golafshan, E. Vorndran, S. Zaharievski, H. Brommer, F. B. Kadumudi, A. Dolatshahi-Pirouz, U. Gbureck, R. van Weeren, M. Castilho and J. Malda, *Biomaterials*, 2020, **261**, 120302.
220 J. W. Kim, B. E. Yang, S. J. Hong, H. G. Choi, S. J. Byeon, H. K. Lim, S. M. Chung, J. H. Lee and S. H. Byun, *Int. J. Mol. Sci.*, 2020, **21**, 4837.
221 Y. H. Wei, D. Y. Zhao, Q. L. Cao, J. Wang, Y. H. Wu, B. Yuan, X. F. Li, X. N. Chen, Y. Zhou, X. Yang, X. D. Zhu, C. Q. Tu and X. D. Zhang, *ACS Biomater. Sci. Eng.*, 2020, **6**, 1787–1797.
222 S. Bose, D. Banerjee, S. Robertson and S. Vahabzadeh, *Ann. Biomed. Eng.*, 2018, **46**, 1241–1253.
223 C. T. Wu, W. Fan, Y. H. Zhou, Y. X. Luo, M. Gelinsky, J. Chang and Y. Xiao, *J. Mater. Chem.*, 2012, **22**, 12288–12295.
224 L. Le Guehennec, V. Dorien, E. Plougonven, G. Nolens, B. Verlee, M. C. De Pauw and F. Lambert, *J. Biomed. Mater. Res., Part A*, 2020, **108**, 412–425.
225 I. I. Bozo, R. V. Deev, I. V. Smirnov, A. Y. Fedotov, V. K. Popov, A. V. Mironov, O. A. Mironova, A. Y. Gerasimenko and V. S. Komlev, *Int. J. Bioprint.*, 2020, **6**, 275.

